HHS Public Access

Author manuscript

Glia. Author manuscript; available in PMC 2024 March 01.

Published in final edited form as:

Glia. 2023 March ; 71(3): 742–757. doi:10.1002/glia.24308.

LPAR1 and aberrantly expressed LPAR3 differentially promote the migration and proliferation of malignant peripheral nerve sheath tumor cells

SHANNON WEBER DOUTT[1,2], **JODY FROMM LONGO**[1], **STEVEN L. CARROLL**[1]

[1]Department of Pathology and Laboratory Medicine, Medical University of South Carolina, Charleston, SC 29425

[2]Medical Scientist Training Program, Medical University of South Carolina, Charleston, SC 29425

Abstract

Schwann cell-derived neoplasms known as malignant peripheral nerve sheath tumors (MPNSTs) are the most common malignancy and the leading cause of death in individuals with neurofibromatosis type 1. Using genome-scale shRNA screens, we have previously found evidence suggesting that lysophosphatidic acid receptors (LPARs) are essential for MPNST proliferation and/or survival. Here, we examine the expression and mutational status of all six LPA receptors in MPNSTs, assess the role that individual LPA receptors play in MPNST physiology and examine their ability to activate key neurofibromin-regulated signaling cascades. We found that human Schwann cells express *LPAR1* and *LPAR6*, while MPNST cells express predominantly *LPAR1* and *LPAR3*. Whole exome sequencing of 16 MPNST cell lines showed no evidence of mutations in any *LPAR* genes or *ENPP2*, a gene encoding a major LPA biosynthetic enzyme. Oleoyl-LPA, an LPA variant with an unsaturated side chain, promoted MPNST cell proliferation and migration. *LPAR1* knockdown ablated the promigratory effect of LPA, while *LPAR3* knockdown decreased proliferation. Inhibition of R-Ras signaling with a doxycycline-inducible dominant negative (DN) R-Ras mutant, which inhibits both R-Ras and R-Ras2, blocked LPA's promigratory effect. In contrast, DN R-Ras did not affect migration induced by neuregulin-1β (NRG1β), suggesting that LPA and NRG1β promote MPNST migration via distinct pathways. LPA-induced migration was also inhibited by Y27632, an inhibitor of the ROCK1/2 kinases that mediate R-Ras effects in MPNSTs. Thus, *LPAR1* and aberrantly expressed *LPAR3* mediate distinct effects in MPNSTs. These receptors and the signaling pathways that they regulate are potentially useful therapeutic targets in MPNSTs.

Graphical Abstract

Address correspondence to: Steven L. Carroll, MD, PhD, Professor and Chair, Department of Pathology and Laboratory Medicine, Medical University of South Carolina, 171 Ashley Avenue, MSC 908, Charleston, SC 29425-9080, Phone: (843) 792-3121, Fax: (843) 792-0555, carrolst@musc.edu.

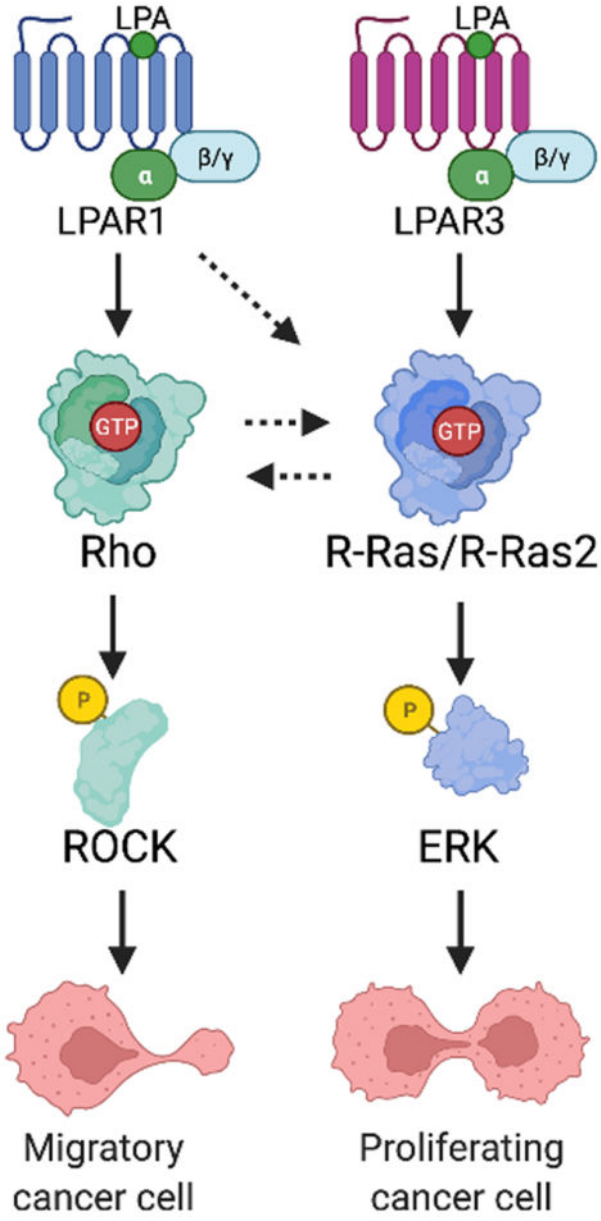

- LPAR3 is aberrantly expressed in MPNST cells, together with LPAR1.
- LPAR1 is uniformly required for LPA-induced MPNST cell migration, while proliferation is predominantly mediated by LPAR3.
- LPA enhanced MPNST migration is mediated by R-Ras proteins and is ROCK dependent.

Keywords

Neurofibromatosis; sarcoma; bioactive lipids; G-protein coupled receptors; R-Ras proteins; peripheral nervous system

1 | INTRODUCTION

Aggressive Schwann cell-derived neoplasms known as malignant peripheral nerve sheath tumors (MPNSTs) are the most common malignancy and the leading cause of death in individuals with the tumor susceptibility syndrome neurofibromatosis type 1 (NF1) (Carroll, 2012). MPNSTs also occur sporadically in the general population and at sites of previous radiotherapy. At present, surgical resection is the only effective means of treating MPNSTs as currently utilized radio- and chemotherapeutic regimens have little, if any effect, on these neoplasms. To identify new therapeutic targets in MPNSTs, we performed genome-scale shRNA screens (Turney-Ivey et al, in preparation). These screens implicated several proteins in the proliferation and/or survival of MPNST cell lines, including receptors for the lipid lysophosphatidic acid (LPA).

At present, little is known regarding LPA effects on MPNSTs. However, LPA is known to play important roles in Schwann cell physiology. LPA, acting through lysophosphatidic acid receptor 1 (LPAR1), promotes embryonic Schwann cell migration, myelination, and axon segregation (Anliker et al., 2013). LPA also activates LPAR1 to promote the survival, but not the proliferation, of cultured neonatal Schwann cells (Li et al., 2003; Weiner & Chun, 1999). In keeping with this, mice with genetic ablation of *Lpar1* show increased Schwann cell apoptosis during their first postnatal week (Contos, Fukushima, Weiner, Kaushal, & Chun, 2000). In contrast, LPA is a potent mitogen for adult Schwann cells (Frohnert, Stonecypher, & Carroll, 2003c). LPA also induces changes in Schwann cell morphology by modifying the structure of the actin cytoskeleton and promoting both laminin-mediated cell adhesion and the formation of cell-cell junctions containing N-cadherin (Weiner, Fukushima, Contos, Scherer, & Chun, 2001).

Some previous observations are consistent with the suggestion that LPA promotes MPNST pathogenesis. NF1-associated MPNSTs and their benign precursors, plexiform neurofibromas, have inactivating mutations of the *NF1* gene which encodes the Ras GTPase activating protein (GAP) neurofibromin; loss of neurofibromin in MPNSTs results in hyperactivation of multiple classic Ras proteins [H-Ras, K-Ras and N-Ras (Brossier et al., 2015)], R-Ras and R-Ras2 (Weber et al., 2021). LPA likely acts at least in part through neurofibromin-regulated signaling cascades as LPA effects on Schwann cell proliferation and survival are enhanced in *Nf1*-null Schwann cells compared to wild-type cells (Nebesio et al., 2007). Further, *ENPP2*, a gene that encodes the LPA-synthesizing enzyme autotaxin (ATX), is in a chromosomal region that is amplified in a subset of MPNSTs (Frank, Gunawan, Holtrup, & Fuzesi, 2003; Hennig, Loschke, Katenkamp, Bartnitzke, & Bullerdiek, 2000; Schmidt et al., 2000). It is also notable that LPA contributes to the pathogenesis of several types of human cancers (Balijepalli, Sitton, & Meier, 2021; Xu, 2019) including neoplasms arising in breast (Du et al., 2010; Samadi, Bekele, Goping, Schang, & Brindley, 2011), prostate (Harma et al., 2011; Ward et al., 2011), colon (Leve et al., 2011), ovary (Kim et al., 2011; Wu, Mukherjee, Lebman, & Fang, 2011), skin (Jankowski, 2011), liver (Zhang et al., 2011), stomach (Bennett, Sadlier, Doran, Macmathuna, & Murray, 2011) and brain (Annabi, Lachambre, Plouffe, Sartelet, & Beliveau, 2009; Hoelzinger et al., 2008). These observations have led to the development of small molecular inhibitors of LPARs and ATX

that are being evaluated for their effectiveness against several of these tumor types (Lin, Lin, & Chen, 2021; Meduri et al., 2021; Schleicher et al., 2011).

Based on these observations, we hypothesized that LPA, acting through one or more of the six LPA receptors, promotes MPNST pathogenesis. To test this hypothesis, we examined the expression and mutational status of all six LPA receptors in surgically resected MPNSTs, MPNST cell lines and wild-type Schwann cells, the effects that LPA and specific LPA receptors exert on proliferation, survival and migration and the ability of LPA and its receptors to activate key neurofibromin-regulated Ras signaling cascades that are essential for MPNST pathogenesis.

2 | MATERIALS AND METHODS

2.1 | Reagents and antibodies

Oleoyl (18:1)-LPA was purchased from Avianti Polar Lipids (Alabaster, AL; # 857128X). The LPAR1/3 inhibitor Ki16425 (#10012659) was purchased from Cayman Chemical Company (Ann Arbor, MI) and the selective ROCK1/2 inhibitor Y26732 was from Selleckchem (#S6390). See Table S1 for a list of the antibodies, primers, and short hairpin RNAs used in this study. Fluorescein isothiocyanate (FITC)- and horseradish peroxidase-conjugated donkey anti-mouse and anti-rabbit secondary antibodies were purchased from Jackson Immunoresearch (West Grove, PA). Enhanced chemiluminescence reagents were from Thermo Scientific Pierce Protein Biology Products (Rockford, IL).

2.2 | MPNST cell lines

We have previously described the sources of the NF1-associated ST88-14, NMS2, NMS2-PC, 90.8TL, S462, T265-2c, MPNST2, MPNST642, NSF1, sNF02.2, sNF94.3 and sNF96.2 and the sporadic STS-26T, HS-PSS and HsSch2 human MPNST cell lines used in this study (Byer et al., 2011; Eckert, Byer, Clodfelder-Miller, & Carroll, 2009; Longo et al., 2019; Stonecypher, Byer, Grizzle, & Carroll, 2005). The 2XSB sporadic MPNST cell line was derived and characterized in our laboratory (Longo et al., 2021). Non-neoplastic human Schwann cells were purchased from ScienCell Research Laboratories (Carlsbad, CA). Inducible R-Ras dominant negative mutants were made as previously described (Brossier et al., 2015; Weber et al., 2021). Cell lines were propagated in DMEM10 [Dulbecco's modification of Eagle's medium (DMEM) containing 10% heat-inactivated fetal calf serum (FCS), 10 IU/mL penicillin and 10 μg/mL streptomycin]. For serum deprived experiments, cells were grown in 0.01-0% serum containing media for 16–24 hours. Cell lines were regularly tested for *Mycoplasma* infection and their morphology and doubling times were checked at regular intervals. Karyotypic analyses showed that these cell lines contained only human chromosomes, ruling out the possibility that they were contaminated with non-human cells.

2.3 | Human specimens

Experiments using human tissues were reviewed and approved by the University of Alabama at Birmingham (UAB) and the Medical University of South Carolina (MUSC) Institutional Review Boards for Human Use. Surgically resected MPNST tumor samples were obtained

from the Southern Division of the Cooperative Human Tissue Network and the UAB Comprehensive Cancer Center Tissue Procurement Shared Facility. Formalin-fixed paraffin embedded tumor specimens were retrieved from the files of the UAB Department of Pathology and the MUSC Department of Pathology and Laboratory Medicine.

2.4 | RNA-Seq and whole exome sequencing analyses

Total RNA was isolated using standard Trizol based methods from primary human Schwann cells, MPNST cell lines and surgically resected MPNST specimens. RNA integrity was verified on an Agilent 2200 TapeStation (Agilent Technologies, Palo Alto, CA); samples with RINs ≥8 were used for sequencing. RNA-Seq libraries were prepared from total RNA (100–200 ng) using a TruSeq RNA Sample Prep Kit per the manufacturer's protocol (Illumina, San Diego, CA). Libraries were clustered at a concentration that ensured at least 50 million reads per sample on a cBot as described by the manufacturer (Illumina, San Diego, CA). Clustered RNA-Seq libraries were then sequenced using Version 4 with 1×50 cycles on an Illumina HiSeq2500. Demultiplexing was performed utilizing bcl2fastq-1.8.4 to generate Fastq files. RNA from three biological replicates was sequenced. Sequencing reads (single end reads, 50 million depth) were aligned using DNAStar software (Madison WI). Partek Genomics Suite (Partek, Inc.; St. Louis MO) and DNAStar software were used to identify statistically significant expression changes of at least 1.5-fold up or down compared to controls.

To perform whole exome sequencing, genomic DNA was isolated from cell pellets using a QIAamp DNA Blood Mini Kit (Qiagen, Inc., Valencia CA; #51104) per the manufacturer's recommendations. Genomic DNA was fragmented by sonication and then purified using Agencourt AMPure XP beads (Agencourt BioSciences Corporation, Beverly MA). Exome capture and library construction was performed using a SureSelectXT Human All Exon Kit (Agilent Technologies, Santa Clara CA), with index tags added by amplification of the captured exome. Whole exome paired-end sequencing (100 bp sequenced from each end) was performed using an Illumina HiSeq2000 instrument. Quality metrics for sequencing datasets were determined with FastQC (Babraham Bioinformatics), with only datasets that received passing scores for all metrics proceeding to further analysis. The datasets with passing quality metrics were analyzed using two distinct pipelines and the results from each pipeline compared to each other. In the first pipeline, sequence reads were aligned to the human reference genome GRCh37/hg19 using DNASTAR SeqMan NGen software (version 15.0.0), and in the second pipeline, Varsome was used. Known and novel single nucleotide polymorphisms (SNPs) and small indels were identified using both platforms to ensure reproducibility and confidence.

2.5 | Immunocytochemistry and immunohistochemistry

Immunohistochemistry was performed per our previously published protocol (Longo et al., 2019) with the following modifications: citrate buffer (pH 6.0, Vector #H-3300) was used for antigen retrieval in a steam cooker for 25 min and endogenous peroxidase activity was blocked for 10 min using 1.5% hydrogen peroxide in Milli-Q purified water. LPAR1 (Abcam #ab166903) and LPAR3 (Abcam #137497) primary antibodies, diluted 1:25, were incubated on slides overnight in a humidified chamber at 4°C. Following incubation with

secondary antibodies, Vector Labs' DAB protocol was followed with HRP reactions being incubated for 2 min (LPAR1) or 7 min (LPAR3 and non-immune IgG). All brightfield images were taken on an Olympus BX53 microscope with a DP80 dual CCD camera and CellSens imaging software.

For immunocytochemistry, cells were plated at 14,000 cells/well in 8-well chamber slides. The next day, cells were washed 3X in PBS and then fixed for 18 minutes with 4% paraformaldehyde in PBS at room temperature (RT). After washing cells 3X in PBS, aldehydes were quenched in fresh 50 mM NH_4Cl/PBS $MgCl_2$ for 10 minutes at RT and then permeabilized with 0.3% Triton X-100 for 15 minutes at RT. Cells were then washed 3X with PBS before being blocked with 5% normal goat serum in PBS for 1 hour at RT. Cells were incubated with primary antibodies (LPAR1: NBPI-03363, NBP1-00788, R&D MAB9963; LPAR3: ab137497, Bioss bs-2882R; PM marker: ab7671) overnight at 4°C. The following day, cells were washed 3X in PBS and then incubated with secondary antibodies and phalloidin stain for 1 hour at RT. 30 minutes after beginning this 1-hour incubation, Hoechst counterstain (2.5 ug/ml) was added to each well. Cells were then washed 3X in PBS and mounted in Invitrogen Prolong Diamond. Slides were cured overnight at RT prior to imaging as described above. Single Z-stack images were acquired on Zeiss Axio M2 using 0.13 μm × 0.13 μm × 0.5 μm sampling (MicroBrightField software) with an 63X × 1.4 NA plan apochromat oil immersion objective.

2.6 | RNA interference

Sigma shRNA lentiviral vectors (Table S1) were obtained from the MUSC Hollings Cancer Center shRNA Technology Shared Resource. Virus was generated by infecting HEK 293T cells with shRNA vectors and MISSION® shRNA Lentiviral Packaging Mix (Sigma product #SHP001) following the protocol in the MISSION® shRNA user manual. Transfections were performed in the presence of antibiotic-free DMEM10. Viral supernatant was harvested 24 hours post-transfection and 1mL aliquots were prepared and stored at −80°C for future use.

MPNST cells were infected with lentiviruses using a reverse transduction protocol. Cells were harvested and seeded into 60cm dishes (300,000 cells/dish) with 0.5mL of virus-containing supernatant, 1.5mL of DMEM10, and polybrene at a final concentration of 10μg/mL. Puromycin selection was initiated 48 hours following transduction. Cells were selected for at least 72 hours after the addition of puromycin before validation of knockdown by RT-PCR.

2.7 | DNA synthesis assays

Cells maintained in serum-free Schwann cell defined media (Frohnert et al., 2003c), were challenged with varying concentrations of LPA. 48 hours later, ^{3}H-thymidine incorporation assays were performed as previously described (Byer et al., 2011). Sixteen replicates were counted per condition.

2.8 | Celigo cytometer proliferation assays

A Celigo® Imaging Cytometer (Nexcelom Bioscience; Lawrence MA) was used to perform proliferation assays. For these assays, cells were plated at 2000 cells/well in 100μL of DMEM10 in a Falcon® 96-well plate and allowed to adhere overnight. The following day, 100μL of Hoescht 33258 was added to each well and incubated for 30 mins. Each well was then imaged using programmed autofocusing to gather Day 1 baselines; this was performed using "Direct Cell Counting" (Blue [ex: 377/50 nm, em: 470/22 nm]) to quantitatively assess the number of nuclei post-Hoescht 33258 staining and brightfield imaging for cell morphology analysis. Plates were reimaged as described above at days 3, 5 and 7. Proliferation curves were calculated using Prism version 8.0.0 for Windows (GraphPad Software; San Diego CA).

2.9 | Transwell migration assays

Cell lines stably transfected with a doxycycline-inducible DN R-Ras or enhanced green fluorescent protein (eGFP) vector (Weber et al., 2021) were maintained for 48 hours in tetracycline-free DMEM-10 supplemented with vehicle or 2 μg/mL doxycycline. These, as well as other lines whose migratory responses were being tested, were then cultured in Schwann cell-defined medium (Frohnert, Stonecypher, & Carroll, 2003a; Frohnert et al., 2003c); in the case of our stably transfected DN R-Ras or eGFP cells, the media was supplemented with vehicle or 2 μg/mL doxycycline. After 24 hours, migration assays were performed on poly-L-lysine/laminin coated Transwell filter inserts (Becton Dickinson Labware) as we previously described (Eckert et al., 2009). For experiments using the ROCK inhibitor Y27632, inhibitor was added 30 minutes after plating so as not to interfere with cell adherence. Filters were stained with 10μg/mL Hoescht 33258 and photographed using fluorescence microscopy at 10x magnification with an EVOS M5000 Imaging System (Thermo Scientific). Cell counts of 9 distinct fields captured from each filter were analyzed and quantified using ImageJ (Schneider, Rasband, & Eliceiri, 2012).

2.10 | Real-time quantitative PCR assays

Real-time quantitative PCR was performed with an ABI 7500 Real Time PCR System (Applied Biosystems, Inc.; Foster City, CA) per our previously described protocol (Stonecypher, Chaudhury, Byer, & Carroll, 2006). Levels of *GAPDH, LPAR1*, *LPAR2*, *LPAR3, LPAR4, LPAR5,* and *LPAR6* cDNAs were determined using TaqMan MGB probes labeled with FAM dye (Table S1). *LPAR* transcript levels were normalized to the levels of *GAPDH* mRNA present in the same specimen. All reactions were performed in triplicate. Controls lacking added template were performed in parallel to verify an absence of contamination. Data were analyzed using the $\Delta\Delta C_t$ methodology with Applied Biosystems Sequence Detection software (version 1.4).

2.11 | Immunoblot analyses

Lysates of human MPNST cells prepared using RIPA lysis buffer were separated by polyacrylamide gel electrophoresis (PAGE), transferred to nitrocellulose and immunoblotted per our previously described methodology (Stonecypher et al., 2006). Blots were reprobed

with an anti-α-actinin antibody to verify equal loading of lanes. An Odyssey Li-Cor Imaging System was used to detect immunoreactive species.

2.12 | Statistical analysis

All experiments were performed and quantified using at least 3 independent biological and technical replicates, with individual replicates indicated in assay descriptions. Data were normalized to uninduced control data and graphs plotted as normalized means ± standard errors of the mean (SEM). *P*-values were calculated using a two-tailed Student t-test, one-way ANOVA or two-way ANOVA as indicated using GraphPad Prism version 8.0.0 for Windows.

3 | RESULTS

3.1 | Oleoyl-LPA variably promotes proliferation and uniformly promotes chemotactic migration in MPNST cells

LPA promotes the migration, but not the proliferation, of neonatal rat Schwann cells (Anliker et al., 2013; Barber, Mellor, Gampel, & Scolding, 2004; Weiner & Chun, 1999). In contrast, we have found that LPA promotes the proliferation of adult rat Schwann cells (Frohnert, Stonecypher, & Carroll, 2003b). These observations raised the question of whether LPA promotes the migration of MPNSTs cells, as is seen with neonatal Schwann cells, and/or their proliferation, as observed with LPA-stimulated adult Schwann cells. To address this question, we challenged two MPNST cell lines derived from NF1-associated MPNSTs (ST88-14 and 90.8TL cells) and a sporadic MPNST cell line (STS-26T cells) with varying concentrations of oleoyl-LPA and examined the effect that this had on DNA synthesis. As serum contains high levels of LPA, adherent MPNST cells were maintained in serum-free medium for 12 hours prior to being challenged for 48 hours with 1 nM to 10 μM concentrations of oleoyl-LPA. Quantification of ^{3}H-thymidine incorporation indicated that 90.8TL cells demonstrated a robust, statistically significant proliferative response (approximately 200% of the level of ^{3}H-thymidine incorporation seen in cells receiving vehicle) to oleoyl-LPA, with peak proliferation achieved with a 10 nM concentration of this lipid (Figure 1a). Oleoyl-LPA had a modest, but statistically significant, proliferative effects in STS-26T cells; as in 90-8TL cells, maximal proliferation was observed with 10 nM LPA. In contrast, oleoyl-LPA did not significantly enhance DNA synthesis in ST88-14 cells.

To determine whether oleoyl-LPA induced the migration of MPNST cells, we performed Transwell migration assays with the same three MPNST cell lines used in our ^{3}H-thymidine incorporation assays. For these experiments, serum-starved MPNST cells were plated on the upper surfaces of Transwell inserts coated with poly-L-lysine and laminin, a combination that we have shown serves as an effective substrate for MPNST cell migration (Eckert et al., 2009). Varying concentrations of oleoyl-LPA or vehicle were then added to the media beneath the Transwell insert and MPNST cells allowed to migrate for 6 hours, a time that we have previously found to be optimal for Transwell migration assays with MPNST cells (Eckert et al., 2009). All three cell lines showed statistically significant and dose-dependent increases in migration in the presence of oleoyl-LPA (Figure 1b). However, the concentration of oleoyl-LPA that maximally induced migration differed from line to line.

ST88-14 cells showed the most robust response, with 100 nM and 1 μM oleoyl-LPA both producing migration that was over 300% greater than that seen with cells challenged with vehicle. In contrast, 1 μM and 10 μM oleoyl-LPA maximally induced migration in 90.8TL cells, with rates that were over 250% of what we observed in cells challenged with vehicle. STS-26T cell migration was greatest with 100 nM oleoyl-LPA, which induced migration that was approximately 200% of what we observed in vehicle treated cells. Oleoyl-LPA thus had potent migratory effects on all three of the lines that we tested.

To determine whether oleoyl-LPA promoted MPNST cell migration in a chemokinetic (enhancement of non-directed movement) or a chemotactic (enhancement of movement towards a higher LPA concentration) manner, we performed Transwell migration assays in which oleoyl-LPA was placed in the lower chamber only, the upper chamber only or both chambers and compared the relative rate of migration under these conditions. These experiments were performed using ST88-14 cells with 1 μM oleoyl-LPA, the concentration of this lipid that maximally induced ST88-14 migration. We found that 1 μM oleoyl-LPA again produced migration that was over 300% compared to the vehicle control when it was present in the bottom chamber (Figure 2). In contrast, this same concentration of LPA only modestly increased migration when present in the top chamber only or when present in both chambers. We conclude that LPA promotes MPNST cell migration in a chemotactic manner.

3.2 | MPNST cells express LPAR1 and aberrantly express LPAR3

Lysophosphatidic acid (LPA) activates six different receptors [LPAR 1–6] (Bandoh et al., 2000; Yanagida & Ishii, 2011), each of which can activate heterotrimeric GTP-binding proteins (G-proteins) that regulate myriad cellular functions. As an initial step towards determining which receptors mediate LPA effects on proliferation and migration, we performed RNA-Seq on non-neoplastic human Schwann cells and the human MPNST cell lines used in our migration and ^{3}H-thymidine incorporation assays. We then compared the relative levels of expression of all six LPA receptor mRNAs within each sample (Figure 3a). We found that non-neoplastic Schwann cells expressed predominantly *LPAR1* and *LPAR6* transcripts. In contrast, ST88-14 and STS-26T MPNST cells expressed predominantly *LPAR1* and *LPAR3* mRNAs; *LPAR6* expression was markedly lower in both lines. *LPAR1* and *LPAR3* transcripts similarly predominated in 90.8TL MPNST cells, with lower levels of *LPAR2* and *LPAR4* mRNAs additionally present. Quantitative PCR assessing the expression of LPAR1-6 in these lines demonstrated transcript level profiles similar to those seen with RNA-Seq (Figure S1).

To determine whether *LPAR1* and/or *LPAR3* expression was consistently elevated in MPNST cells relative to non-neoplastic Schwann cells, we performed RNA-Seq on an additional 10 NF1-associated human MPNST cell lines (T265-2c, MPNST2, MPNST642, NMS2, NMS2-PC, NSF1, sNF02.2, S462, sNF94.3, sNF96.2) and three more sporadic human MPNST cell lines (2XSB, HS-PSS, HsSch2). We then used DESeq2 analyses to compare *LPAR1* and *LPAR3* mRNA levels in non-neoplastic Schwann cells to those evident in these 16 MPNST cell lines. The expression of *LPAR1* transcripts was variable, with increased expression seen only in 90.8TL, sNF02.2, sNF94.3 and sNF96.2 lines (Figure 3b). In contrast, *LPAR3* expression was significantly increased in 12 of the 16 MPNST cell lines

that we examined (Figure 3b, asterisks); NSF1 and 2XSB cells were the only two MPNST lines that showed reduced *LPAR3* expression.

We next asked whether LPAR1 and/or LPAR3 mediated LPA effects in non-neoplastic human Schwann cells and MPNST cells. Our genome-scale shRNA screens had previously implicated LPAR3 in proliferation (also, see below). Consequently, we focused on the effect that the competitive LPAR1/3 inhibitor Ki16425 had on migration (Figure 3c). In these experiments, cells were challenged with vehicle or the oleoyl-LPA concentration that optimally promoted migration, in the presence or absence of 10 μM Ki16425. We found that Ki16425 treatment resulted in a statistically significant reduction in the baseline migration of human Schwann cells and 90.8TL cells. Ki16425 also completely abolished the effect that oleoyl-LPA exerted on Schwann cell and MPNST cell migration. This indicates that LPAR1 and/or LPAR3 mediate oleoyl-LPA enhanced migration of these cells.

To examine the distribution of LPAR1 and LPAR3 in MPNST cells, we performed double label immunocytochemistry in which ST88-14 and STS-26T cells were stained with antibodies recognizing LPAR1 and LPAR3 (Figure 4). We found strong LPAR1 and LPAR3 immunoreactivity throughout the cells and the distribution of LPAR1 and LPAR3 partially overlapped. However, LPAR1 immunoreactivity was also concentrated in specific juxtanuclear sub-domains in both cell lines. To determine if LPAR1 and LPAR3 were specifically associated with the plasma membrane, we assessed the distribution of LPAR1 and LPAR3 using two different primary antibodies that target distinct regions of each protein together with a plasma membrane-specific maker (Figure 5, Figure S2 and data not shown). As expected for dynamic proteins, we found that LPAR1 and LPAR3 co-localized with the plasma membrane as well as in distinct cytoplasmic and perinuclear sub-cellular regions. The partial colocalization of LPAR1 and LPAR3 raised the question of whether LPAR1 and LPAR3 might regulate different biologic activities in MPNST cells (see below).

To determine whether LPAR1 and/or LPAR3 expression is similarly evident in MPNSTs *in vivo*, we performed immunohistochemistry on six surgically resected MPNSTs. We detected prominent LPAR1 immunoreactivity in all six tumors (Figure 6; Figure S3). This immunoreactivity displayed a diffuse staining pattern consistent with cytoplasmic and plasma membrane association and within juxtanuclear structures. Strong immunoreactivity for LPAR3 was also detected in three of the six tumor specimens (Figure 6a; Figure S3a, b) and was present in a distribution that was highly similar to that of LPAR1, except for a lack of juxtanuclear staining. The remaining three MPNSTs showed no evidence of LPAR3 immunoreactivity (Figure 6b; Figure S3c, d).

To determine whether potentially activating mutations were present in the genes encoding LPARs, we performed whole exome sequencing on all sixteen MPNST cell lines. An exhaustive search showed no evidence of mutations in any of the genes encoding the six LPA receptors. Since a genomic region containing the *ENPP2* (autotaxin) locus is amplified in a subset of MPNSTs, we also performed DESeq2 analyses to compare the expression of *ENPP2* transcripts in human Schwann cells to that seen in these MPNST cell lines. We found elevated *ENPP2* expression only in NMS2 cells (Figure S4). In all the other MPNST cell lines, *ENPP2* expression was decreased compared to non-neoplastic Schwann cells. Our

whole exome sequencing analyses also showed no evidence of mutations in *ENPP2* in any of the 16 MPNST cell lines.

3.3 | LPAR1 mediates LPA-induced MPNST migration while proliferation is dependent upon LPAR3

Since Ki16425 inhibits both LPAR1 and LPAR3, it was unclear whether one or both of these receptors mediate LPA-promoted MPNST cell migration. To establish the function(s) mediated by these receptors, we used shRNAs to knock down the expression of *LPAR1* and *LPAR3* in ST88-14 and STS-26T cells and examined the effect that this had on their migration. Quantitative real-time PCR assays demonstrated that the shRNAs used effectively reduced *LPAR1* and *LPAR3* mRNA levels in ST88-14 and STS-26T cells relative to the levels seen in cells transfected with a non-targeting control (Figure S5). In both cell lines, knockdown of *LPAR1* resulted in a drastic reduction in the migration of cells challenged with vehicle, while *LPAR3* knockdown had no significant effect on migration (Figure 7a). Further, following *LPAR1* knockdown, stimulation with oleoyl-LPA no longer resulted in increased cellular migration in either ST88-14 or STS-26T cells. In contrast, cells in which *LPAR3* expression had been knocked down demonstrated migratory responses to oleoyl-LPA that were similar to those seen in cells transfected with the non-targeting shRNA control. We conclude that LPAR1 promotes both baseline and LPA-stimulated migration of MPNST cells.

To determine whether LPAR1 and/or LPAR3 promote MPNST proliferation, we transduced ST88-14 and STS-26T cells with lentiviral vectors expressing shRNAs that targeted mRNAs encoding these receptors and examined the effect that this had on the proliferation of unstimulated cells over 7 days. We found that the proliferation of ST88-14 cells transduced with *LPAR1* shRNA-expressing vectors was not significantly different from the proliferation of cells transfected with the non-targeting control (Figure 7b). However, knockdown of *LPAR1* expression did produce a modest, but still statistically significant reduction in the number of STS-26T cells by 7 days post-transduction. The distinct NF1 status between these two lines may explain the differential dependence of LPAR1 in mediating proliferation. In contrast, *LPAR3* knockdown robustly reduced the proliferation of both ST88-14 and STS-26T cells (Figure 7c). These findings indicate that aberrantly expressed LPAR3 predominantly drives the baseline proliferation of these MPNST cell lines. However, in STS-26T cells, LPAR1 also contributes to proliferation.

3.4 | LPA induced migration is dependent on R-Ras subfamily signaling and the RhoA/ROCK signaling pathway

Using a doxycycline-inducible dominant negative R-Ras mutant (DN R-Ras), we have previously shown that the migration of unstimulated MPNST cells is dependent on signaling by R-Ras proteins (Weber et al., 2021). This led us to ask whether the increased level of migration seen in LPA-stimulated MPNST cells is similarly dependent on the action of R-Ras proteins. To answer this question, we performed Transwell migration assays with ST88-14 and STS-26T cells that were stably transfected with a doxycycline-inducible DN R-Ras (S43N) mutant which simultaneously inhibits the activation of both R-Ras and R-Ras2. As seen in our earlier work, induction of DN R-Ras expression with doxycycline

reduced the migration of unstimulated cells, albeit it to different degrees (Figure 8a, b). Further, when these cells are challenged with the concentration of oleoyl-LPA that optimally induced their migration, expression of the DN R-Ras mutant prevented an LPA-induced increase in migration. We conclude that LPA-induced MPNST cell migration is dependent on the action of R-Ras and/or R-Ras2.

As an initial step towards identifying the pro-migratory signaling pathways impeded by DN R-Ras expression, we challenged ST88-14 (Fig. 8c) and STS-26T (Figure 8d) with vehicle or oleoyl-LPA and examined the effect that DN R-Ras expression had on the phosphorylation of ERK and AKT, two signaling molecules that we have previously implicated in neuregulin-1β (NRG1β)-stimulated MPNST cell migration (Eckert et al., 2009). In the absence of DN R-Ras expression, we found that LPA promoted the phosphorylation of ERK, but not AKT. In contrast, LPA did not enhance ERK phosphorylation in the presence of DN R-Ras. The observation that LPA did not promote AKT phosphorylation led us to hypothesize that LPA and NRG1β utilize different signaling pathways to promote migration. As an initial test of this hypothesis, we challenged ST88-14 (Fig. 8e) and STS-26T (Fig. 8f) cells with 10 nM NRG1β in the presence and absence of DN R-Ras expression and assessed the effect that this had on their migration. We found that in the absence of DN R-Ras expression, NRG1β potently induced the migration of ST88-14 and STS-26T cells. Intriguingly, however, we also observed that expression of DN R-Ras had no significant effect on migration induced by NRG1β. These observations indicate that NRG1β-induced MPNST cell migration is not dependent on R-Ras signaling; that is distinctly different from the MPNST cell migration promoted by oleoyl-LPA, which is dependent upon the action of R-Ras proteins.

We have shown that ROCK is a key effector of R-Ras/R-Ras2 mediated migration in unstimulated MPNST cells (Weber et al., 2021). Since LPA-induced MPNST cell migration is dependent upon R-Ras signaling, we next asked whether LPA-induced migration of these cells also requires ROCK activation. To test this, we challenged non-neoplastic human Schwann cells (HSC) and three human MPNST cell lines (ST88-14, STS-26T and 90.8TL) with vehicle or the concentration of oleoyl-LPA that optimally promotes their migration in the presence or absence of the selective ROCK inhibitor Y27632. We found that Y27632 treatment abolished the pro-migratory effect of oleoyl-LPA stimulation in all three MPNST cells lines tested, with the STS-26T sporadic line being the least sensitive to ROCK inhibition of LPA stimulated migration (Figure 9a). Curiously, however, Y27632 did not produce a significant decrease in the migration of non-transformed human Schwann cells (Figure 9a).

The observation that ROCK inhibition differentially affected the migration of Schwann cells and MPNST cells suggested that LPA might differentially activate other key signaling pathways in non-neoplastic and neoplastic Schwann cells. We therefore compared the phosphorylation of ERK and AKT in Schwann cells and three MPNST cell lines (ST88-14, STS-26T, 90.8TL) at various times after stimulation with the concentration of oleoyl-LPA stimulation that maximally promoted the migration of each cell type (Figure 9b). We observed that oleoyl-LPA promoted modest phosphorylation of ERK in two of the three MPNST cell lines and in non-neoplastic Schwann cells under serum deprived conditions and

that this effect on pERK was dependent on the severity of serum deprived conditions with lower serum conditions providing a more robust response in ST-8814 and STS-26T cell lines (data not shown). We observed that LPA stimulation enhanced AKT phosphorylation in all three MPNST cell lines; however, in comparing the results from five different replications, we observed the degree to which AKT phosphorylation was enhanced appeared to vary depending on the serum batch that was used for culturing cells (data not shown). We also found that LPA promoted AKT phosphorylation in non-neoplastic human Schwann cells. These observations indicate that LPA activation of the PI3K/AKT signaling pathway in human MPNST cells is complex and context dependent.

4 | DISCUSSION

We have shown that oleoyl-LPA promotes the proliferation of two of the three MPNST cell lines that we tested and the migration of all three lines, acting in a chemotactic manner. In contrast to non-neoplastic human Schwann cells, which predominantly express the LPA receptors LPAR1 and LPAR6, MPNST cells express LPAR1 and LPAR3 that is localized in the cell membrane and in juxtanuclear intracellular compartments. We found that surgically resected MPNSTs also expressed LPAR1 and LPAR3 and that these proteins were expressed in a pattern similar to what we observed in cultured MPNST cells. In keeping with the fact that the LPAR1/LPAR3 inhibitor Ki16425 potently inhibited baseline and LPA-promoted MPNST cell migration, we found that knockdown of LPAR1 expression reduced the basal rate of MPNST cell migration and prevented oleoyl-LPA induced migration, while LPAR3 knockdown had no effect on basal or LPA-induced migration. In contrast, LPAR3 knockdown potently reduced MPNST cell proliferation, even in ST88-14 cells, which did not show a proliferative response to exogenous LPA. The migration of MPNST cells is likely dependent upon the action of R-Ras and/or R-Ras2 as basal and LPA-induced migration is prevented by the expression of an R-Ras DN mutant. The R-Ras DN mutant also blocks the phosphorylation of ERK, a kinase that we have previously implicated in MPNST migration. Our finding that Y27632, an inhibitor of ROCK1/2, prevents LPA-induced migration in MPNST cells and combined with our previous findings of an activated R-Ras - pROCK signaling cascade implicates ROCK in MPNST migration. Considered together, these observations provide interesting new insights into the role that LPA signaling plays in MPNST biology. However, they also raise new questions about the significance of the differences in non-neoplastic and neoplastic Schwann cell expression of LPA receptors, how these receptors are activated in MPNSTs, and how differential receptor expression factors into the distinct biologic and signaling responses we observed following LPA stimulation.

Although MPNST cells express both LPAR1 and LPAR3, only LPAR3 was consistently overexpressed in MPNST cells, with *LPAR3* mRNA expression being elevated in 75% (12/16) of the MPNST cell lines that we examined. Likewise, LPAR3 expression was evident in 50% (3/6) of the MPNST tumor samples that we examined. LPAR1 expression was also evident in all 16 MPNST cell lines and all 6 of the MPNST tumor samples that we analyzed. In contrast to MPNST cells, non-neoplastic human Schwann cells express predominantly LPAR1 and LPAR6. These observations imply that the acquisition of LPAR3 expression is beneficial to MPNSTs, a suggestion that is consistent with our demonstration that knocking down LPAR3 expression diminishes the proliferation of these tumor cells.

Although LPAR1 and LPAR3 are both LPA receptors, it is known that these receptors differ in their ability to activate key signaling cascades in other settings. LPAR1, but not LPAR3, acts through the $G\alpha_{12/13}$ small GTP-binding proteins (G-proteins) to activate RhoA signaling; this latter observation is consistent with our finding that LPAR1 mediates basal and LPA-induced MPNST cell migration, and that this migration is dependent upon ROCK (see below). In contrast, LPAR3 predominantly acts through $G\alpha_{q/11}$ proteins, which activate phospholipase C (PLC). LPAR1 and LPAR3 are both capable of signaling through $G\alpha_{i}$ as well to activate PLC, Ras and PI-3-kinase and to inhibit adenylate cyclase (Chun, Hla, Lynch, Spiegel, & Moolenaar, 2010; Etienne-Manneville & Hall, 2002; Neves, Ram, & Iyengar, 2002). When expressed in insect cells, LPA acts through LPAR3 to increase calcium mobilization; this is not seen with LPAR1 in the same setting (Bandoh et al., 1999). LPAR1 and LPAR3 also differ in their responsiveness to different forms of LPA. LPAR3 is most responsive to LPA with unsaturated side chains, such as the oleoyl-LPA used in this study, while LPAR1 is more broadly responsive, responding to LPA with saturated or unsaturated side chains (Bandoh et al., 2000).

It is also notable that MPNST cells have markedly reduced expression of LPAR6 compared to non-neoplastic Schwann cells. At present, it is unclear what, if any, advantage is conferred on MPNST cells by their markedly reduced expression of LPAR6. However, LPAR6 also has distinct functional characteristics, which suggests that the reduction of LPAR6 expression in MPNST cells is biologically significant. Although LPAR6 (also known as P2Y5) is a *bona fide* LPA receptor, it, unlike LPAR1 and LPAR3, is a member of the purinoreceptor family. Compared to LPAR1 and LPAR3, LPAR6 requires higher concentrations of LPA for activation and it prefers 2-acyl-LPA for activation over 1-acyl-LPA (Kihara, Maceyka, Spiegel, & Chun, 2014). In future experiments, it will be of interest to reintroduce LPAR6 expression in MPNST cells and determine how this alters the physiology of these cells.

Exogenous oleoyl-LPA significantly increased the proliferation of STS-26T and 90.8TL cells, but not that of ST88-14 cells. However, when we knocked down the expression of LPAR3 in ST88-14 and STS-26T cells, we found that proliferation was markedly reduced in both LPA-responsive STS-26T cells and the LPA-nonresponsive ST88-14 line. This suggests that exogenous LPA does not further enhance the proliferation of ST88-14 cells because LPAR3 is already strongly activated in these cells. As we found no evidence of *LPAR3* mutations in any of the 16 MPNST cell lines that we examined, this cannot be the result of activating *LPAR3* mutations. LPA is present in at high concentrations in blood, likely as a result of release from platelets (Benton, Gerrard, Michiel, & Kindom, 1982). Consequently, events such as intratumoral hemorrhage likely generate LPA that promotes MPNST growth *in vivo*. However, our proliferation assays were performed in serum-free medium precisely to avoid this confounding issue. We considered the possibility that elevated ENPP2 expression in MPNST cells results in endogenous LPA production that promotes LPAR3 activation in an autocrine or paracrine fashion. We found, though, that *ENPP2* mRNA levels are decreased in MPNST cells relative to non-neoplastic Schwann cells, which argues that endogenous LPA expression resulting from increased autotaxin expression is unlikely to account for the baseline activation of LPAR3 in MPNST cells. We cannot yet rule out the possibility that other LPA biosynthetic pathways are inappropriately

activated in MPNST cells. Alternatively, it is known that LPA receptors and other GPCRs can be transactivated by receptor tyrosine kinases [RTKs (Kilpatrick & Hill, 2021)], which raises the question of whether LPAR3 is similarly transactivated by one or more RTKs in MPNST cells. This latter possibility merits further exploration as pharmacologic inhibitors are available for several RTKs; these inhibitors could be effective as therapeutic agents for MPNSTs, alone or in combination with currently available LPAR inhibitors.

In contrast to what is seen following LPAR3 knockdown, baseline and LPA-induced migration is markedly reduced following knockdown of LPAR1 in MPNST cells. This aligns with previous studies showing that LPAR1 is a major mediator of migration and other biological activities in Schwann cells (Anliker et al., 2013). LPAR1 activation has also been similarly linked to pathologic migration and metastasis in several other cancer types including pancreatic, ovarian, and colonic adenocarcinomas (Fukushima et al., 2018; Komachi et al., 2009; Takahashi et al., 2017; Yu, Zhang, & Chen, 2016). Our demonstration that LPAR1 and LPAR3 mediate largely distinct events in MPNST physiology also implies that these two LPA receptors activate distinct downstream signaling pathways in these cells; we would note that our observation that LPAR1 knockdown in STS-26T cells modestly reduced proliferation may indicate that there is a partial overlap in the signaling pathways regulated by LPAR1 and LPAR3 in some MPNSTs. In future studies, it will be of interesting to identify and compare the signaling pathways that are regulated downstream of both LPA receptors in MPNST cells.

We found that the promigratory effect of LPA is blocked by the expression of a dominant negative R-Ras mutant which we have shown abolishes the activation of R-Ras and R-Ras2 but not classic Ras proteins (H-Ras, N-Ras, K-Ras) in MPNST cells (Brossier et al., 2015; Weber et al., 2021). Induction of DN R-Ras expression in both ST88-14 and STS-26T cells also blocked the increase in ERK phosphorylation normally seen with LPA stimulation, suggesting that Raf is activated downstream of R-Ras and/or R-Ras2. As we have previously shown that ERK activation is essential for migration induced by another pro-migratory factor, NRG1β, in MPNST cells (Eckert et al., 2009), we then asked whether the DN R-Ras mutant similarly inhibited migration induced by NRG1β. To our surprise, we found that the DN R-Ras mutant had no effect on NRG1β-induced migration of either ST88-14 or STS-26T cells. This indicates that LPA-induced migration is dependent upon R-Ras and/or R-Ras, while migration induced by NRG1β is not dependent on the action of these small G-proteins. We would note that this does not rule out the possibility that ERK phosphorylation is also required for LPA-induced migration. However, it does appear that different growth factors can utilize more than one signaling pathway to promote the migration of MPNST cells.

We were also intrigued to find that LPA could promote the phosphorylation of AKT, another protein that we have previously implicated in NRG1β-induced MPNST cell migration (Eckert et al., 2009). In contrast, human Schwann cells did show an increase in AKT phosphorylation following stimulation of these cells with oleoyl-LPA. This raises the question of whether the expression of LPAR1 and LPAR3 in MPNST cells versus LPAR1 and LPAR6 in Schwann cells is the basis for these different patterns of AKT activation. However, this notion conflicts with previous reports that LPAR3 is capable of activating the

PI-3-kinase/AKT signaling pathway (see above). Consequently, another possibility that will need to be considered is whether other abnormalities downstream of LPAR1 and/or LPAR3 are responsible for these observations. This reinforces the suggestion made above that it will be highly interesting to define the signaling pathways downstream of the different LPA receptors in MPNSTs and non-neoplastic Schwann cells.

In summary, we have found that MPNST express LPAR1 in combination with aberrantly expressed LPAR3. These two LPA receptors mediate distinct effect in MPNST cells and potentially play an important role in tumor cell mitogenesis and invasion *in vivo*. These findings suggest that LPAR3 and LPAR1 may be important new therapeutic targets in MPNSTs. Although we have begun to delineate the signaling pathways downstream of these receptors, our findings are raising a number of intriguing new questions including whether LPAR3 is transactivated by receptor tyrosine kinases or via other mechanisms; the answer to this question will have important therapeutic implications. Further, we have uncovered evidence that non-neoplastic Schwann cells and MPNST cells demonstrate intriguing differences in how LPA affects key cytoplasmic signaling pathways and that LPA and other pro-migratory factors may act through distinct signaling pathways to promote MPNST migration. In future studies, it will be highly informative to compare and contrast the signaling pathways activated by LPA and NRG1βin Schwann cells and MPNST cells.

Supplementary Material

Refer to Web version on PubMed Central for supplementary material.

Acknowledgements:

The authors declare no conflicts of interest. This work was supported by the National Institute of Neurological Diseases and Stroke (R01 NS048353, R01 NS109655), the National Cancer Institute (R01 CA122804, F30 CA247139), the Department of Defense (X81XWH-09-1-0086, W81XWH-12-1-0164, W81XWH-14-1-0073 and W81XWH-15-1-0193) and the Children's Tumor Foundation (2015-05-007 and 2016-04-001).

REFERENCES

Anliker B, Choi JW, Lin ME, Gardell SE, Rivera RR, Kennedy G, & Chun J (2013). Lysophosphatidic acid (LPA) and its receptor, LPA1 , influence embryonic schwann cell migration, myelination, and cell-to-axon segregation. Glia, 61(12), 2009–2022. doi:10.1002/glia.22572 [PubMed: 24115248]

Annabi B, Lachambre MP, Plouffe K, Sartelet H, & Beliveau R (2009). Modulation of invasive properties of CD133+ glioblastoma stem cells: a role for MT1-MMP in bioactive lysophospholipid signaling. Molecular carcinogenesis, 48(10), 910–919. doi:10.1002/mc.20541 [PubMed: 19326372]

Balijepalli P, Sitton CC, & Meier KE (2021). Lysophosphatidic Acid Signaling in Cancer Cells: What Makes LPA So Special? Cells, 10(8). doi:10.3390/cells10082059

Bandoh K, Aoki J, Hosono H, Kobayashi S, Kobayashi T, Murakami-Murofushi K, … Inoue K (1999). Molecular cloning and characterization of a novel human G-protein-coupled receptor, EDG7, for lysophosphatidic acid. J Biol Chem, 274(39), 27776–27785. doi:10.1074/jbc.274.39.27776 [PubMed: 10488122]

Bandoh K, Aoki J, Taira A, Tsujimoto M, Arai H, & Inoue K (2000). Lysophosphatidic acid (LPA) receptors of the EDG family are differentially activated by LPA species. Structure-activity relationship of cloned LPA receptors. FEBS letters, 478(1–2), 159–165. [PubMed: 10922489]

Barber SC, Mellor H, Gampel A, & Scolding NJ (2004). S1P and LPA trigger Schwann cell actin changes and migration. Eur J Neurosci, 19(12), 3142–3150. doi:10.1111/j.0953-816X.2004.03424.x [PubMed: 15217370]

Bennett G, Sadlier D, Doran PP, Macmathuna P, & Murray DW (2011). A functional and transcriptomic analysis of NET1 bioactivity in gastric cancer. BMC Cancer, 11, 50. doi:10.1186/1471-2407-11-50 [PubMed: 21284875]

Benton AM, Gerrard JM, Michiel T, & Kindom SE (1982). Are lysophosphatidic acids or phosphatidic acids involved in stimulus activation coupling in platelets? Blood, 60(3), 642–649. [PubMed: 6921047]

Brossier NM, Prechtl AM, Longo JF, Barnes S, Wilson LS, Byer SJ, … Carroll SL (2015). Classic Ras Proteins Promote Proliferation and Survival via Distinct Phosphoproteome Alterations in Neurofibromin-Null Malignant Peripheral Nerve Sheath Tumor Cells. J Neuropathol Exp Neurol, 74(6), 568–586. doi:10.1097/NEN.0000000000000201 [PubMed: 25946318]

Byer SJ, Eckert JM, Brossier NM, Clodfelder-Miller BJ, Turk AN, Carroll AJ, … Carroll SL (2011). Tamoxifen inhibits malignant peripheral nerve sheath tumor growth in an estrogen receptor-independent manner. Neuro-oncology, 13(1), 28–41. doi:10.1093/neuonc/noq146 [PubMed: 21075781]

Carroll SL (2012). Molecular mechanisms promoting the pathogenesis of Schwann cell neoplasms. Acta Neuropathol, 123(3), 321–348. doi:10.1007/s00401-011-0928-6 [PubMed: 22160322]

Chun J, Hla T, Lynch KR, Spiegel S, & Moolenaar WH (2010). International Union of Basic and Clinical Pharmacology. LXXVIII. Lysophospholipid receptor nomenclature. Pharmacol Rev, 62(4), 579–587. doi:10.1124/pr.110.003111 [PubMed: 21079037]

Contos JJ, Fukushima N, Weiner JA, Kaushal D, & Chun J (2000). Requirement for the lpA1 lysophosphatidic acid receptor gene in normal suckling behavior. Proc Natl Acad Sci U S A, 97(24), 13384–13389. doi:10.1073/pnas.97.24.13384 [PubMed: 11087877]

Du J, Sun C, Hu Z, Yang Y, Zhu Y, Zheng D, … Lu X (2010). Lysophosphatidic acid induces MDA-MB-231 breast cancer cells migration through activation of PI3K/PAK1/ERK signaling. PLoS One, 5(12), e15940. doi:10.1371/journal.pone.0015940 [PubMed: 21209852]

Eckert JM, Byer SJ, Clodfelder-Miller BJ, & Carroll SL (2009). Neuregulin-1 beta and neuregulin-1 alpha differentially affect the migration and invasion of malignant peripheral nerve sheath tumor cells. Glia, 57(14), 1501–1520. doi:10.1002/glia.20866 [PubMed: 19306381]

Etienne-Manneville S, & Hall A (2002). Rho GTPases in cell biology. Nature, 420(6916), 629–635. doi:10.1038/nature01148 [PubMed: 12478284]

Frank D, Gunawan B, Holtrup M, & Fuzesi L (2003). Cytogenetic characterization of three malignant peripheral nerve sheath tumors. Cancer Genet Cytogenet, 144(1), 18–22. [PubMed: 12810251]

Frohnert PW, Stonecypher MS, & Carroll SL (2003a). Constitutive activation of the neuregulin-1/ErbB receptor signaling pathway is essential for the proliferation of a neoplastic Schwann cell line. Glia, 43(2), 104–118. doi:10.1002/glia.10232 [PubMed: 12838503]

Frohnert PW, Stonecypher MS, & Carroll SL (2003b). Lysophosphatidic acid promotes the proliferation of adult Schwann cells isolated from axotomized sciatic nerve. J Neuropathol Exp Neurol, 62(5), 520–529. doi:10.1093/jnen/62.5.520 [PubMed: 12769191]

Frohnert PW, Stonecypher MS, & Carroll SL (2003c). Lysophosphatidic acid promotes the proliferation of adult Schwann cells isolated from axotomized sciatic nerve. Journal of neuropathology and experimental neurology, 62(5), 520–529. [PubMed: 12769191]

Fukushima K, Otagaki S, Takahashi K, Minami K, Ishimoto K, Fukushima N, … Tsujiuchi T (2018). Promotion of cell-invasive activity through the induction of LPA receptor-1 in pancreatic cancer cells. J Recept Signal Transduct Res, 38(4), 367–371. doi:10.1080/10799893.2018.1531889 [PubMed: 30396320]

Harma V, Knuuttila M, Virtanen J, Mirtti T, Kohonen P, Kovanen P, … Nees M (2011). Lysophosphatidic acid and sphingosine-1-phosphate promote morphogenesis and block invasion of prostate cancer cells in three-dimensional organotypic models. Oncogene. doi:10.1038/onc.2011.396

Hennig Y, Loschke S, Katenkamp D, Bartnitzke S, & Bullerdiek J (2000). A malignant triton tumor with an unbalanced translocation (1;13)(q10;q10) and an isochromosome (8)(q10) as the sole karyotypic abnormalities. Cancer Genet Cytogenet, 118(1), 80–82. [PubMed: 10731598]

Hoelzinger DB, Nakada M, Demuth T, Rosensteel T, Reavie LB, & Berens ME (2008). Autotaxin: a secreted autocrine/paracrine factor that promotes glioma invasion. Journal of neuro-oncology, 86(3), 297–309. doi:10.1007/s11060-007-9480-6 [PubMed: 17928955]

Jankowski M (2011). Autotaxin: its role in biology of melanoma cells and as a pharmacological target. Enzyme research, 2011, 194857. doi:10.4061/2011/194857 [PubMed: 21423677]

Kihara Y, Maceyka M, Spiegel S, & Chun J (2014). Lysophospholipid receptor nomenclature review: IUPHAR Review 8. Br J Pharmacol, 171(15), 3575–3594. doi:10.1111/bph.12678 [PubMed: 24602016]

Kilpatrick LE, & Hill SJ (2021). Transactivation of G protein-coupled receptors (GPCRs) and receptor tyrosine kinases (RTKs): Recent insights using luminescence and fluorescence technologies. Curr Opin Endocr Metab Res, 16, 102–112. doi:10.1016/j.coemr.2020.10.003 [PubMed: 33748531]

Kim EK, Park JM, Lim S, Choi JW, Kim HS, Seok H, … Suh PG (2011). Activation of AMP-activated protein kinase is essential for lysophosphatidic acid-induced cell migration in ovarian cancer cells. The Journal of biological chemistry, 286(27), 24036–24045. doi:10.1074/jbc.M110.209908 [PubMed: 21602274]

Komachi M, Tomura H, Malchinkhuu E, Tobo M, Mogi C, Yamada T, … Okajima F (2009). LPA1 receptors mediate stimulation, whereas LPA2 receptors mediate inhibition, of migration of pancreatic cancer cells in response to lysophosphatidic acid and malignant ascites. Carcinogenesis, 30(3), 457–465. doi:10.1093/carcin/bgp011 [PubMed: 19129242]

Leve F, Marcondes TG, Bastos LG, Rabello SV, Tanaka MN, & Morgado-Diaz JA (2011). Lysophosphatidic acid induces a migratory phenotype through a crosstalk between RhoA-Rock and Src-FAK signalling in colon cancer cells. European journal of pharmacology. doi:10.1016/j.ejphar.2011.09.006

Li Y, Gonzalez MI, Meinkoth JL, Field J, Kazanietz MG, & Tennekoon GI (2003). Lysophosphatidic acid promotes survival and differentiation of rat Schwann cells. J Biol Chem, 278(11), 9585–9591. doi:10.1074/jbc.M213244200 [PubMed: 12524451]

Lin YH, Lin YC, & Chen CC (2021). Lysophosphatidic Acid Receptor Antagonists and Cancer: The Current Trends, Clinical Implications, and Trials. Cells, 10(7). doi:10.3390/cells10071629

Longo JF, Brosius SN, Black L, Worley SH, Wilson RC, Roth KA, & Carroll SL (2019). ErbB4 promotes malignant peripheral nerve sheath tumor pathogenesis via Ras-independent mechanisms. Cell Commun Signal, 17(1), 74. doi:10.1186/s12964-019-0388-5 [PubMed: 31291965]

Longo JF, Brosius SN, Znoyko I, Alers VA, Jenkins DP, Wilson RC, … Carroll SL (2021). Establishment and genomic characterization of a sporadic malignant peripheral nerve sheath tumor cell line. Sci Rep, 11(1), 5690. doi:10.1038/s41598-021-85055-2 [PubMed: 33707600]

Meduri B, Pujar GV, Durai Ananda Kumar T, Akshatha HS, Sethu AK, Singh M, … Mathew B (2021). Lysophosphatidic acid (LPA) receptor modulators: Structural features and recent development. Eur J Med Chem, 222, 113574. doi:10.1016/j.ejmech.2021.113574 [PubMed: 34126459]

Nebesio TD, Ming W, Chen S, Clegg T, Yuan J, Yang Y, … Yang FC (2007). Neurofibromin-deficient Schwann cells have increased lysophosphatidic acid dependent survival and migration-implications for increased neurofibroma formation during pregnancy. Glia, 55(5), 527–536. doi:10.1002/glia.20482 [PubMed: 17236191]

Neves SR, Ram PT, & Iyengar R (2002). G protein pathways. Science, 296(5573), 1636–1639. doi:10.1126/science.1071550 [PubMed: 12040175]

Samadi N, Bekele RT, Goping IS, Schang LM, & Brindley DN (2011). Lysophosphatidate induces chemo-resistance by releasing breast cancer cells from taxol-induced mitotic arrest. PLoS One, 6(5), e20608. doi:10.1371/journal.pone.0020608 [PubMed: 21647386]

Schleicher SM, Thotala DK, Linkous AG, Hu R, Leahy KM, Yazlovitskaya EM, & Hallahan DE (2011). Autotaxin and LPA receptors represent potential molecular targets for the radiosensitization of murine glioma through effects on tumor vasculature. PLoS One, 6(7), e22182. doi:10.1371/journal.pone.0022182 [PubMed: 21799791]

Schmidt H, Taubert H, Meye A, Wurl P, Bache M, Bartel F, … Hinze R (2000). Gains in chromosomes 7, 8q, 15q and 17q are characteristic changes in malignant but not in benign peripheral nerve sheath tumors from patients with Recklinghausen's disease. Cancer letters, 155(2), 181–190. [PubMed: 10822134]

Schneider CA, Rasband WS, & Eliceiri KW (2012). NIH Image to ImageJ: 25 years of image analysis. Nat Methods, 9(7), 671–675. doi:10.1038/nmeth.2089 [PubMed: 22930834]

Stonecypher MS, Byer SJ, Grizzle WE, & Carroll SL (2005). Activation of the neuregulin-1/ErbB signaling pathway promotes the proliferation of neoplastic Schwann cells in human malignant peripheral nerve sheath tumors. Oncogene, 24(36), 5589–5605. doi:10.1038/sj.onc.1208730 [PubMed: 15897877]

Stonecypher MS, Chaudhury AR, Byer SJ, & Carroll SL (2006). Neuregulin growth factors and their ErbB receptors form a potential signaling network for schwannoma tumorigenesis. Journal of neuropathology and experimental neurology, 65(2), 162–175. doi:10.1097/01.jnen.0000199575.93794.2f [PubMed: 16462207]

Takahashi K, Fukushima K, Onishi Y, Inui K, Node Y, Fukushima N, … Tsujiuchi T (2017). Lysophosphatidic acid (LPA) signaling via LPA4 and LPA6 negatively regulates cell motile activities of colon cancer cells. Biochem Biophys Res Commun, 483(1), 652–657. doi:10.1016/j.bbrc.2016.12.088 [PubMed: 27993681]

Ward Y, Lake R, Yin JJ, Heger CD, Raffeld M, Goldsmith PK, … Kelly K (2011). LPA Receptor Heterodimerizes with CD97 to Amplify LPA-Initiated RHO-Dependent Signaling and Invasion in Prostate Cancer Cells. Cancer research. doi:10.1158/0008-5472.CAN-11-2381

Weber SM, Brossier NM, Prechtl A, Barnes S, Wilson LS, Brosius SN, … Carroll SL (2021). R-Ras subfamily proteins elicit distinct physiologic effects and phosphoproteome alterations in neurofibromin-null MPNST cells. Cell Commun Signal, 19(1), 95. doi:10.1186/s12964-021-00773-4 [PubMed: 34530870]

Weiner JA, & Chun J (1999). Schwann cell survival mediated by the signaling phospholipid lysophosphatidic acid. Proc Natl Acad Sci U S A, 96(9), 5233–5238. doi:10.1073/pnas.96.9.5233 [PubMed: 10220449]

Weiner JA, Fukushima N, Contos JJ, Scherer SS, & Chun J (2001). Regulation of Schwann cell morphology and adhesion by receptor-mediated lysophosphatidic acid signaling. J Neurosci, 21(18), 7069–7078. [PubMed: 11549717]

Wu J, Mukherjee A, Lebman DA, & Fang X (2011). Lysophosphatidic Acid-Induced p21Waf1 Expression Mediates the Cytostatic Response of Breast and Ovarian Cancer Cells to TGFbeta. Molecular cancer research : MCR, 9(11), 1562–1570. doi:10.1158/1541-7786.MCR-11-0340 [PubMed: 21890597]

Xu Y (2019). Targeting Lysophosphatidic Acid in Cancer: The Issues in Moving from Bench to Bedside. Cancers (Basel), 11(10). doi:10.3390/cancers11101523

Yanagida K, & Ishii S (2011). Non-Edg family LPA receptors: the cutting edge of LPA research. Journal of biochemistry. doi:10.1093/jb/mvr087

Yu X, Zhang Y, & Chen H (2016). LPA receptor 1 mediates LPA-induced ovarian cancer metastasis: an in vitro and in vivo study. BMC Cancer, 16(1), 846. doi:10.1186/s12885-016-2865-1 [PubMed: 27809800]

Zhang R, Zhang Z, Pan X, Huang X, Huang Z, & Zhang G (2011). ATX-LPA axis induces expression of OPN in hepatic cancer cell SMMC7721. Anatomical record, 294(3), 406–411. doi:10.1002/ar.21324

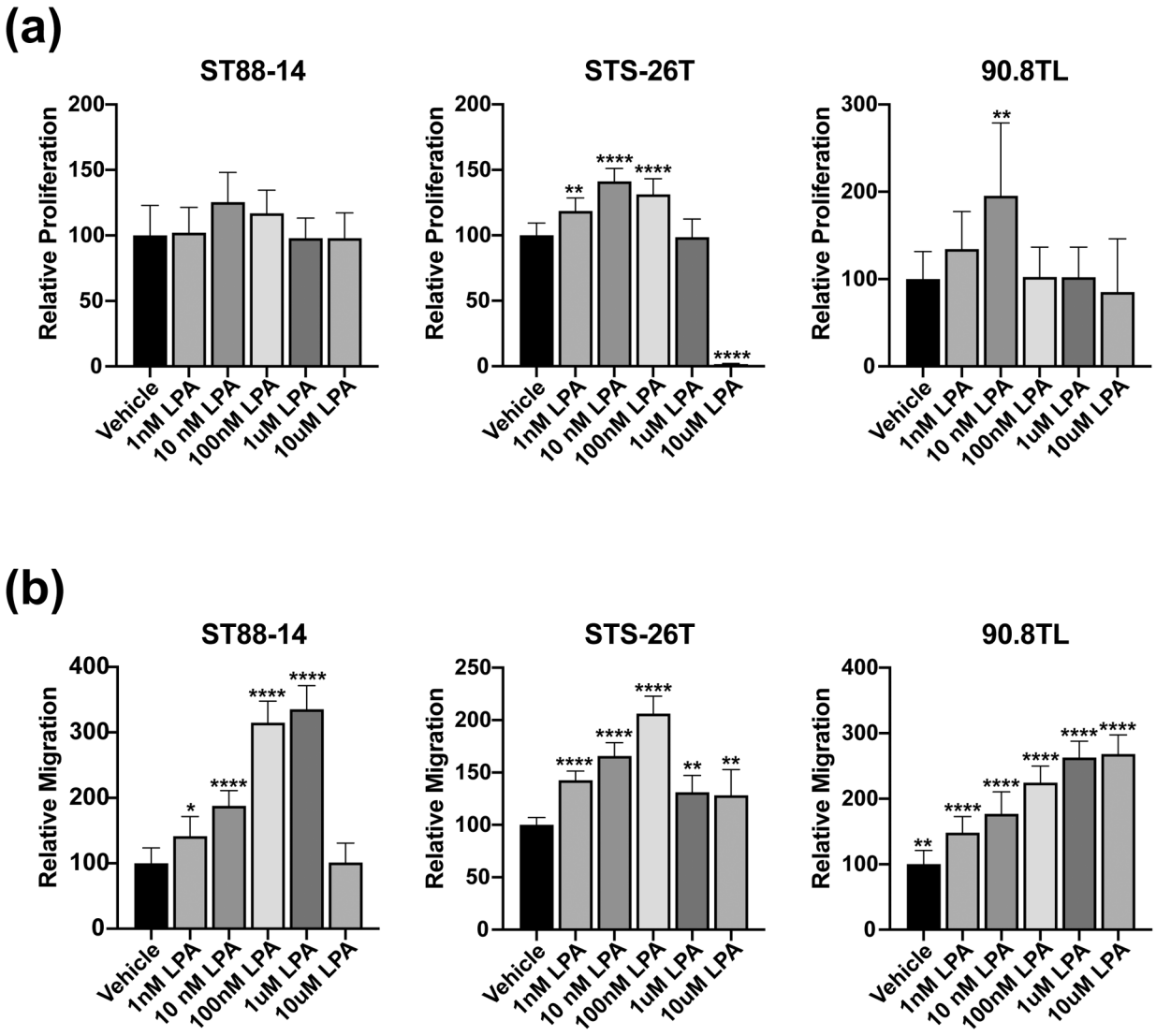

FIGURE 1.

Oleoyl-LPA variably promotes the proliferation and migration of human MPNST cells. (a) ^{3}H-Thymidine incorporation assays in MPNST cell lines challenged with vehicle or varying concentrations (1 nM to 10 μM) of oleoyl-LPA show that this lipid promotes DNA synthesis in STS-26T and 90.8TL cells, with a maximum effect achieved at 10 nM; LPA did not induce statistically significant changes in the proliferation of ST88-14 cells. (b) Transwell migration assays in MPNST cell lines challenged with vehicle or 1 nM to 10 μM concentrations of oleoyl-LPA show that LPA promotes the migration of all three of these cell lines. However, the concentration of oleoyl-LPA that maximally promotes migration is variable from line to line. In both (a) and (b), values are normalized to the levels observed in cells challenged with vehicle. Standard errors of the means are indicated on each bar. * indicates a p-value ≤0.05; ** indicates a p-value ≤0.01; **** indicates a p-value ≤0.0001.

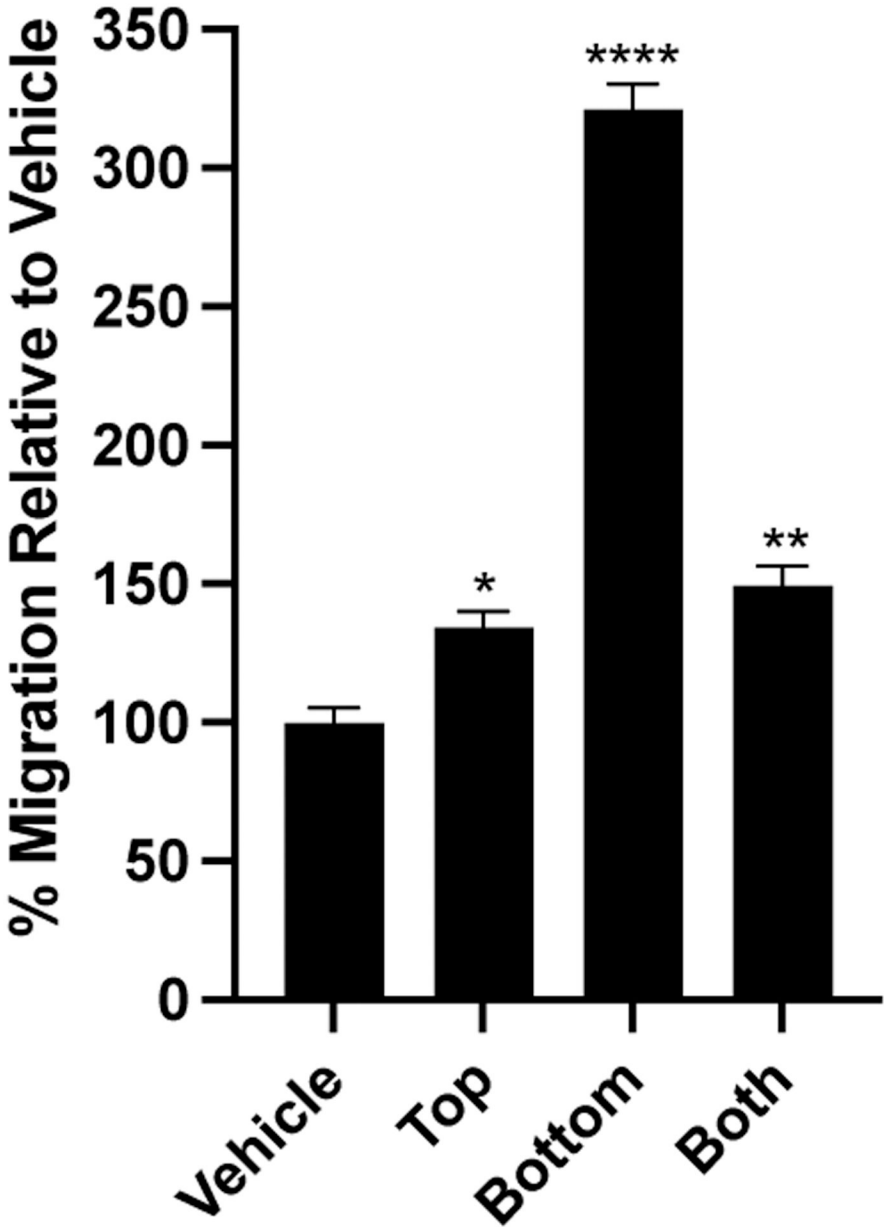

FIGURE 2.

Oleoyl-LPA promotes the migration of ST88-14 MPNST cells in a chemotactic rather than a chemokinetic manner. Cells were plated on the upper surface of poly-L-lysine/laminin coated Transwell inserts. LPA was then added to the top chamber only (Top), bottom chamber only (Bottom) or both the top and bottom chambers (Both) and cells allowed to migrate for 6 hours. Counts of the numbers of cells migrating to the bottom surface of the Transwell insert showed that placing LPA in the bottom chamber induced the great degree of migration. Bars are normalized to the amount of cellular migration in wells receiving vehicle and standard errors of the mean are shown for each condition. * indicates a p-value ≤0.05; ** indicates a p-value ≤0.01; **** indicates a p-value ≤0.0001.

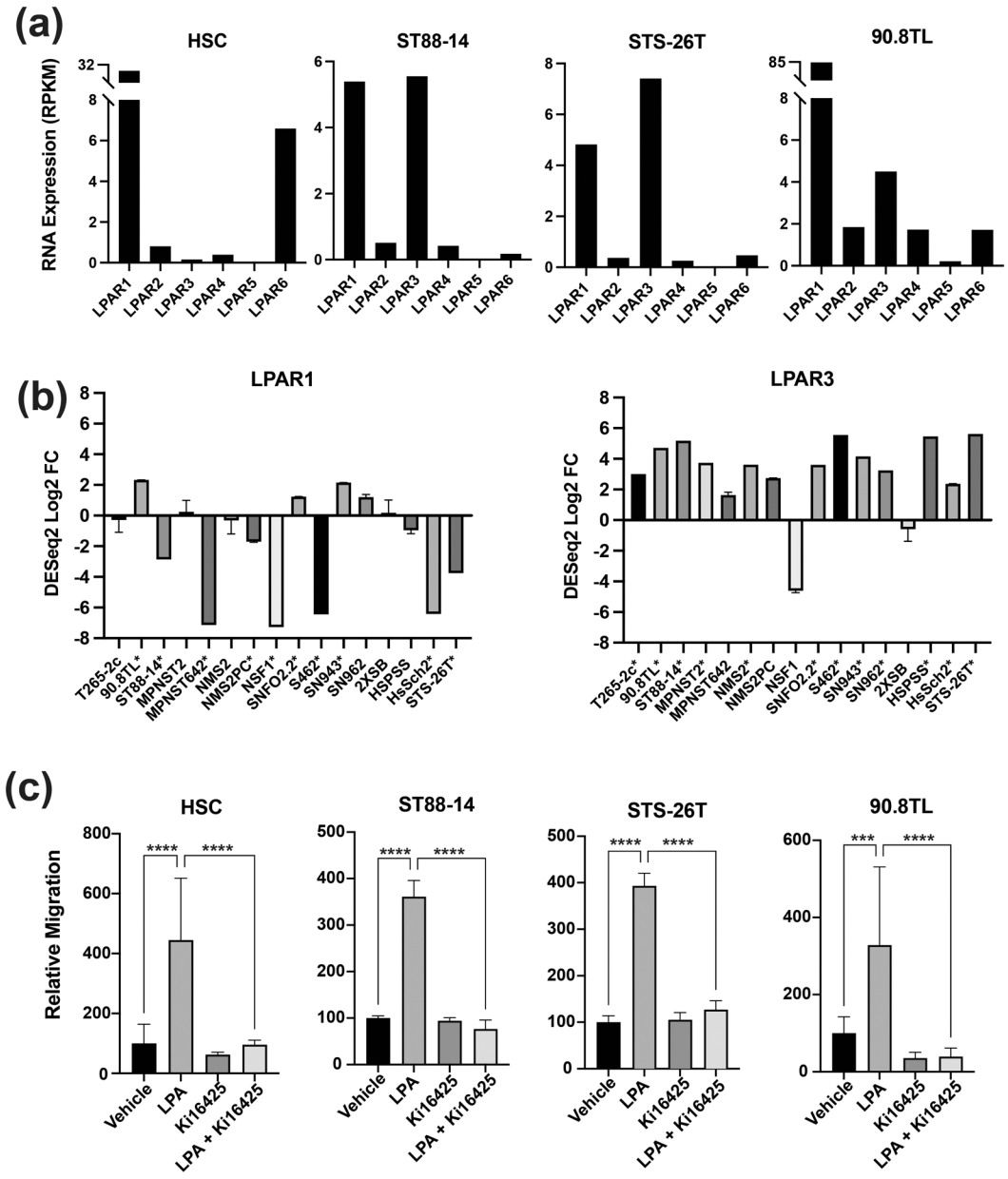

FIGURE 3.

Human MPNST cells express *LPAR1* and *LPAR3* transcripts and an LPAR1/3 inhibitor blocks LPA-induced migration. (a) Comparison of the expression of the different *LPAR* mRNAs in non-neoplastic human Schwann cells (HSC) shows that these glia express predominantly *LPAR1* and *LPAR6* transcripts. In contrast, *LPAR1* and *LPAR3* mRNAs are most abundant in three human MPNST cell lines (ST88-14, STS-26T and 90.8TL). (b) To determine whether *LPAR1* and/or *LPAR3* transcripts are consistently overexpressed in human MPNST cells relative to non-neoplastic Schwann cells, the levels of these transcripts were compared in Schwann cells and a panel of 16 MPNST cell lines. Although *LPAR1* was not consistently overexpressed in MPNST cells, *LPAR3* mRNA levels were significantly elevated in 12 of the 16 lines. * indicates a *p*-value ≤0.05 for the comparison to Schwann

cells. (c) Transwell migration assays were performed with human Schwann cells and MPNST cells challenged with vehicle, the concentration of oleoyl-LPA that maximally induced migration of the tested cells, a 10 μM concentration of the LPAR1/3 inhibitor Ki16425 or LPA in combination with Ki16425. Ki16425 prevented migration induced by LPA. *** indicates a p-value ≤0.001; **** indicates a p-value ≤0.0001.

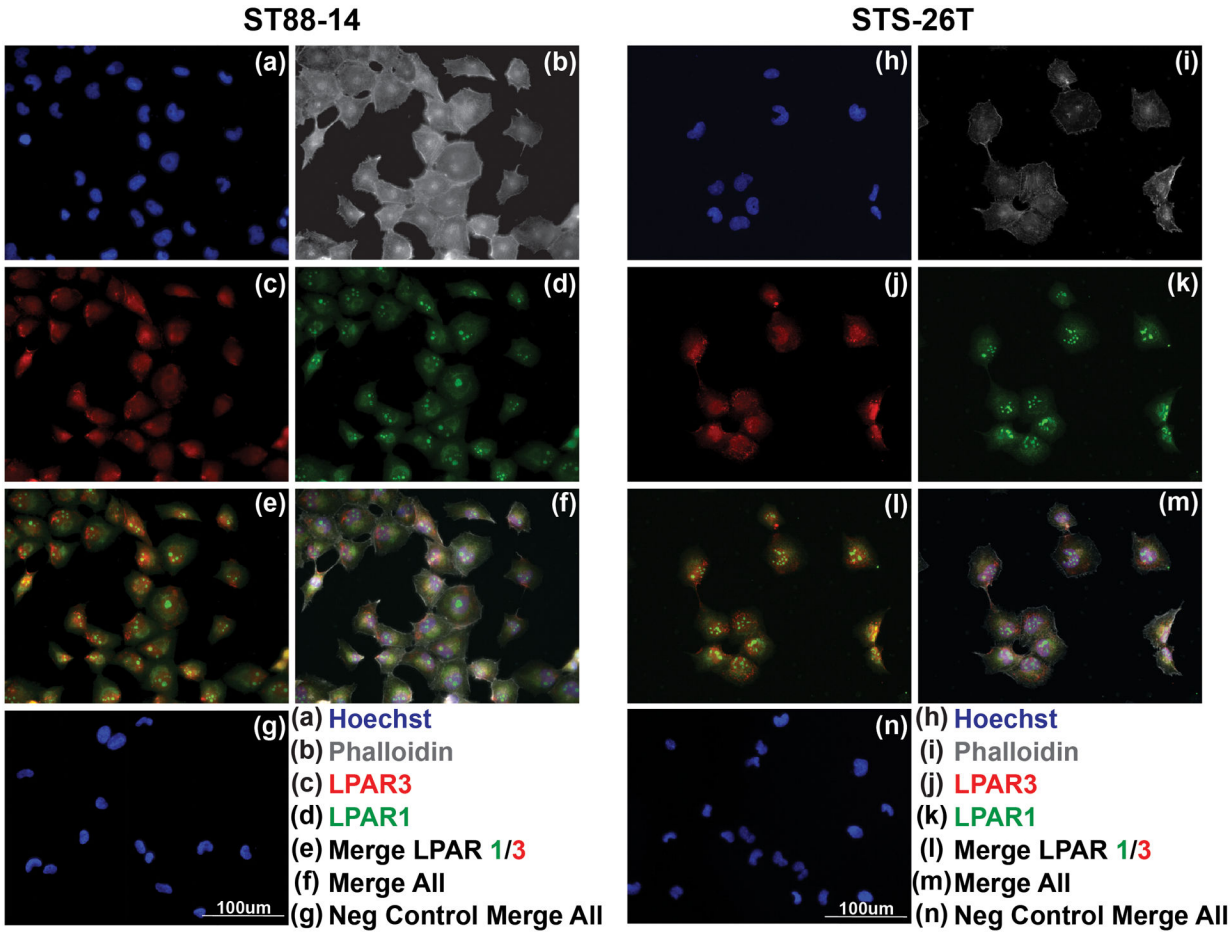

FIGURE 4.

Representative immunocytochemistry images of ST88-14 and STS-26T MPNST cells comparing the distribution of LPAR1 and LPAR3. (a-g) Photomicrographs of the same field of ST88-14 cells demonstrating bisbenzimide stained nuclei (a), the actin cytoskeleton as labeled with phalloidin (b), LPAR3 (c), LPAR1 (d), a merged image of the LPAR1 and LPAR3 stains (e) and a merged image of all of these stains (f). A merged image of all of these stains in preparations in which the LPAR1 and LPAR3 antibodies were replaced with isotype-matched nonimmune antibodies is presented in (g). (h-n) Photomicrographs of the same field of STS-26T cells demonstrating bisbenzimide stained nuclei (h), the actin cytoskeleton as labeled with phalloidin (i), LPAR3 (j), LPAR1 (k), a merged image of the LPAR1 and LPAR3 stains (l) and a merged image of all these stains (m). A merged image of all these stains in preparations in which the LPAR1 and LPAR3 antibodies were replaced with isotype-matched nonimmune antibodies is presented in (n).

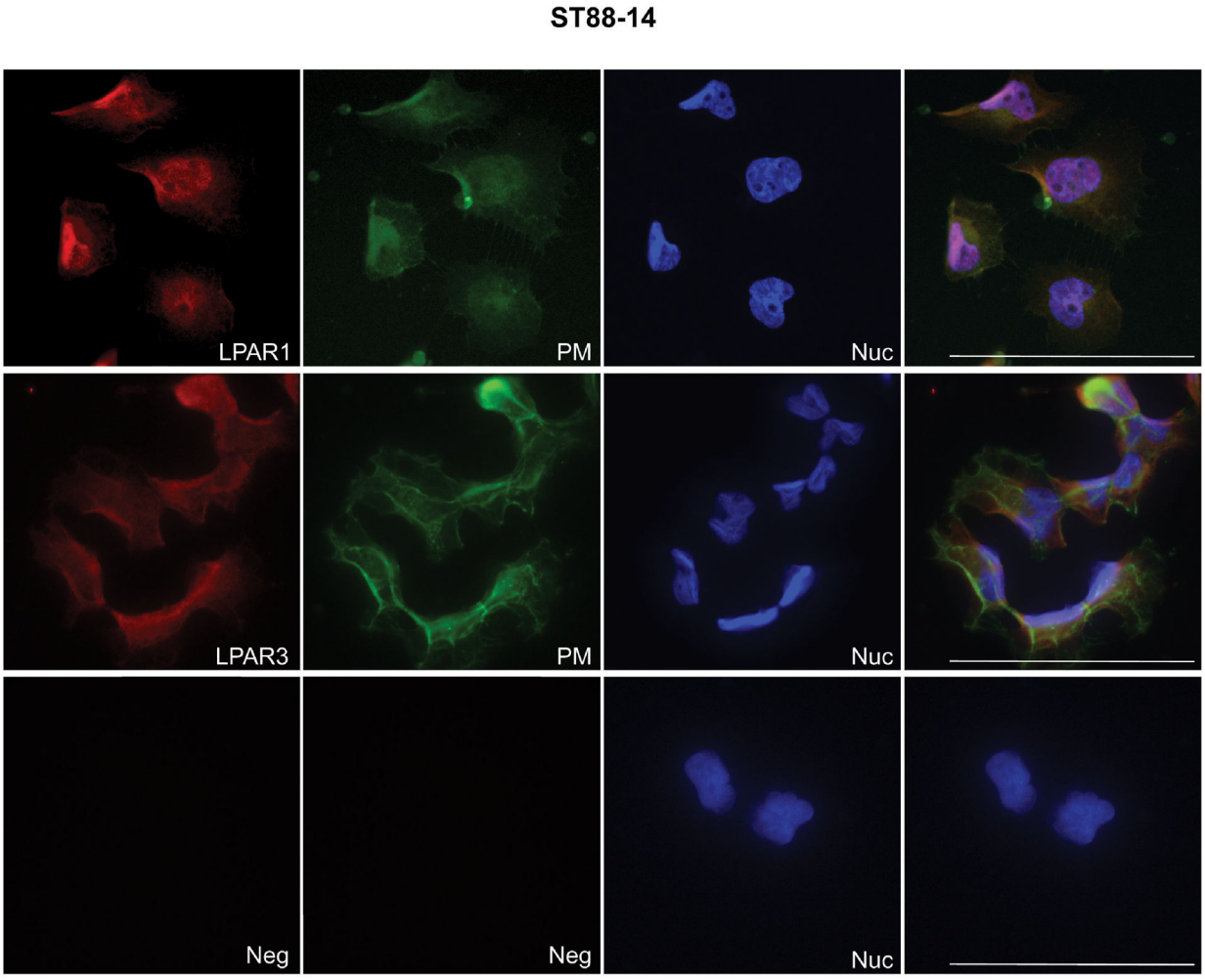

FIGURE 5.

Representative immunocytochemistry images of ST88-14 MPNST cells comparing the distribution of LPAR1 and LPAR3 in relation to a known plasma membrane marker using z-stack microscopy software. Photomicrographs of the same field of cells demonstrating LPAR 1 or LPAR3 stained in red, a plasma membrane marker stained in green, nuclei stained with Hoechst 33342 in blue then together in a merged image of the LPAR/PM/Nuc. For a negative control, a merged image of all these stains in preparations in which the LPAR1 and LPAR3 antibodies were replaced with isotype-matched nonimmune antibodies was performed and presented. Images are merged single z-stack acquisitions and were taken using a 63X objective. Scale bar represents 100 μm.

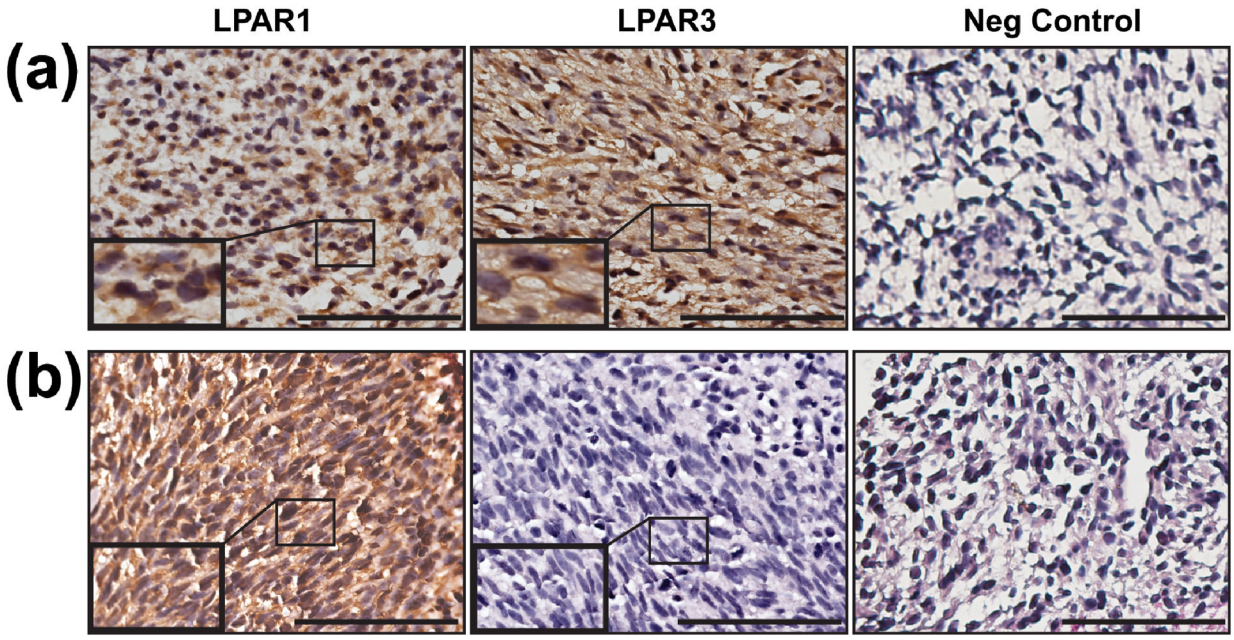

FIGURE 6.

Representative immunohistochemical stains of human formalin-fixed paraffin-embedded NF1-associated MPNSTs demonstrating differential expression of LPAR1 and LPAR3 *in vivo*. **(a)** Representative images of LPAR1 and LPAR3 immunoreactivity in an MPNST that expressed both receptors. **(b)** Representative images of LPAR1 and LPAR3 staining in an MPNST that expressed only LPAR1. Non-immune rabbit IgG served as a negative control (Neg Control). Images were acquired using a 63X primary objective. Scale bars equal 100 μm.

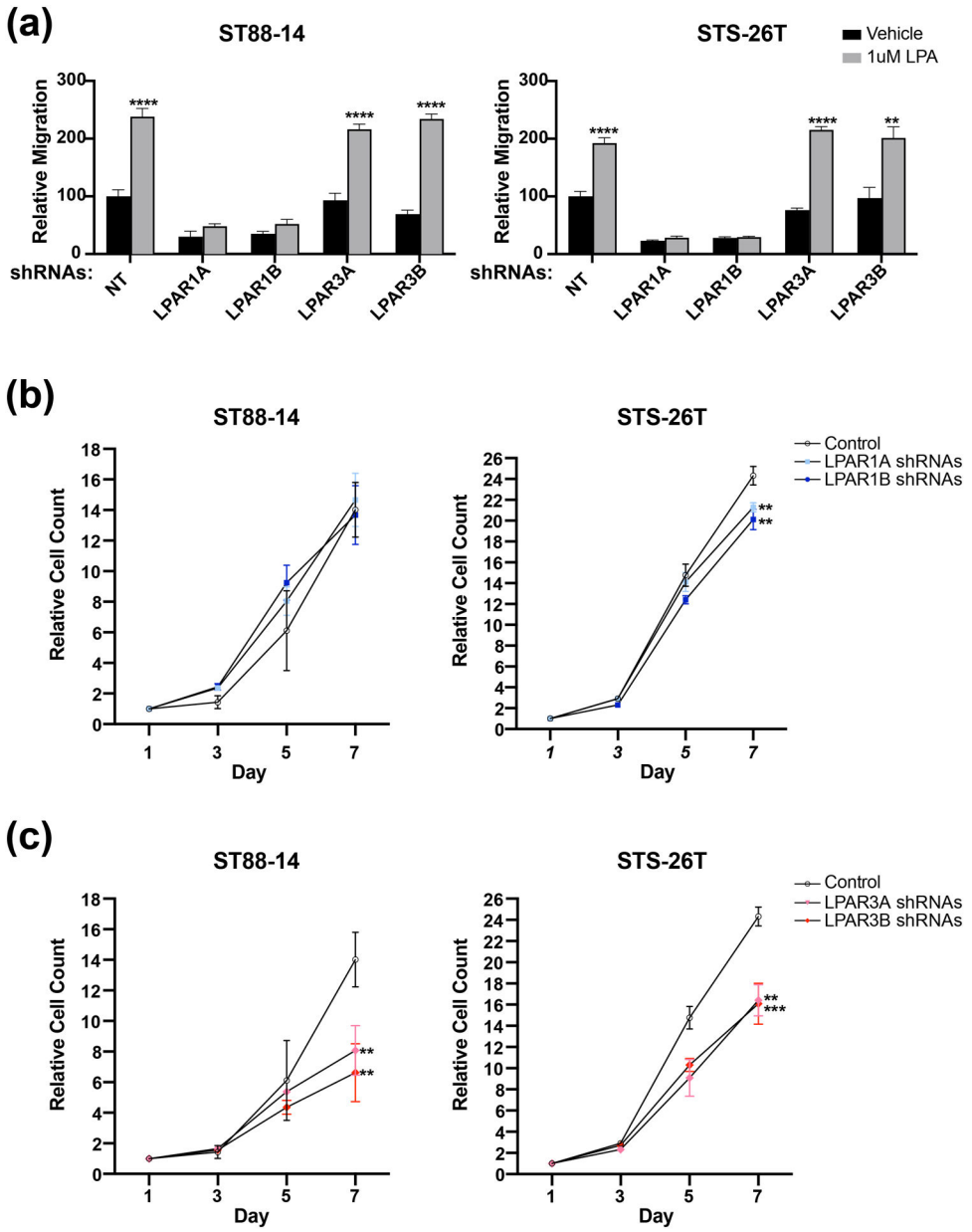

FIGURE 7.

Knockdown of gene expression with shRNAs implicates LPAR1 in the migration of MPNST cells and LPAR3 in their proliferation. (a) Knockdown of *LPAR1*, but not *LPAR3*, reduced baseline migration and prevented LPA-induced migration in ST88-14 and STS-26T cells. Two different shRNAs (A and B) were used for each target. NT indicates cells transfected with a non-targeting control. ** indicates a *p*-value ≤0.01; *** indicates a *p*-value ≤0.001; **** indicates a *p*-value ≤0.0001 for comparison to LPA-induced migration in cells transfected with the non-targeting control. (b) *LPAR1* knockdown had no effect on the proliferation of unstimulated ST88-14 cells but did produce a modest, but still statistically significant reduction in the proliferation of STS-26T cells. (c) Knockdown of LPAR3 expression potently reduced the proliferation of both ST88-14 and STS-26T cells. In

(b) and (c), ** indicates a *p*-value ≤0.01; *** indicates a *p*-value ≤0.001; **** indicates a *p*-value ≤0.0001 for comparisons to cells transfected with the non-targeting control.

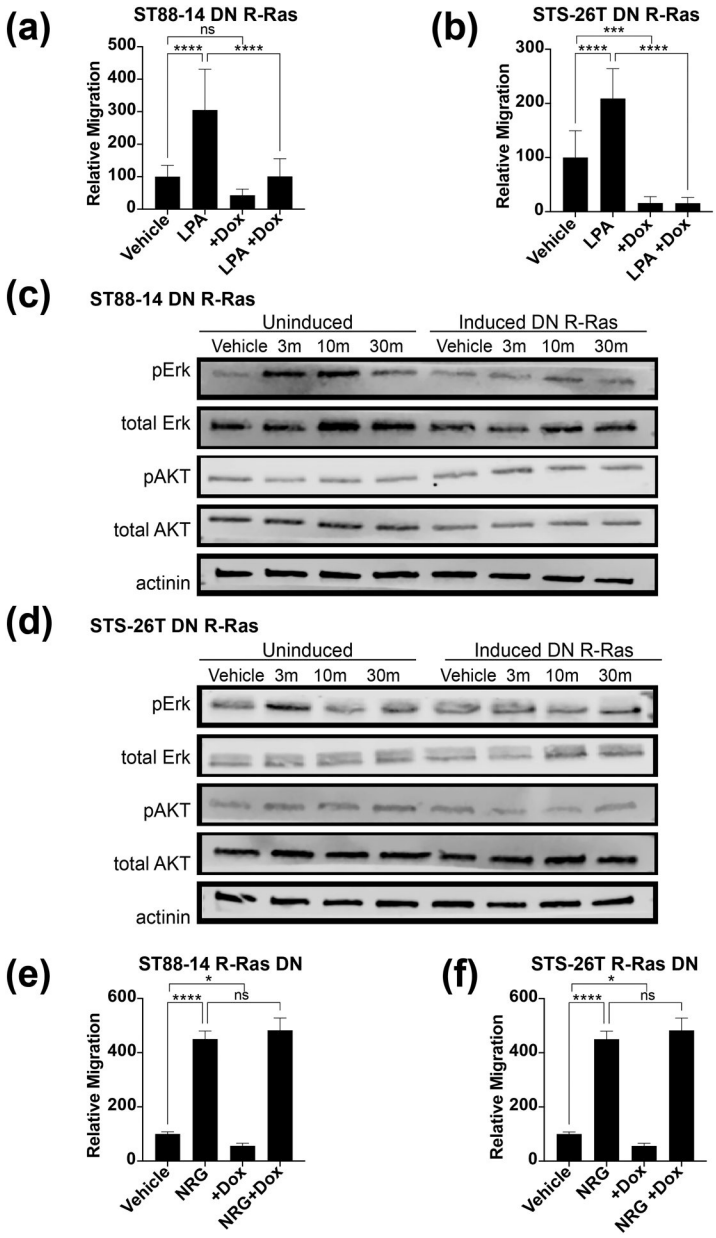

FIGURE 8.

Doxycycline-induced expression of a dominant negative (DN) R-Ras mutant prevents the migration of MPNST cells induced by LPA, but not by neuregulin-1β (NRG1β). (a, b) Doxycycline-induced expression of DN R-Ras prevents LPA-induced increases in the migration of ST88-14 (a) or STS-26T (b) cells. (c, d) ST88-14 (c) and STS-26T (d) cells were challenged with the concentration of LPA that optimally induced their migration in the absence (Uninduced) or presence of DN R-Ras expression and the effects of this stimulation on the phosphorylation of Erk and AKT then examined. In cells in which DN R-Ras expression has not been induced, LPA increases Erk phosphorylation. However, in the presence of DN R-Ras expression increased Erk phosphorylation is prevented. In contrast, LPA has little, if any, effect on AKT phosphorylation, either in the presence or absence of

DN R-Ras expression. (e,f) Unlike what is seen with oleoyl-LPA, DN R-Ras expression does not inhibit NRG1β-induced migration of ST88-14 (e) and STS-26T (f) cells. * indicates *p*-value ≤0.05; *** indicates *p*-value ≤0.001; **** indicates *p*-value ≤0.0001.

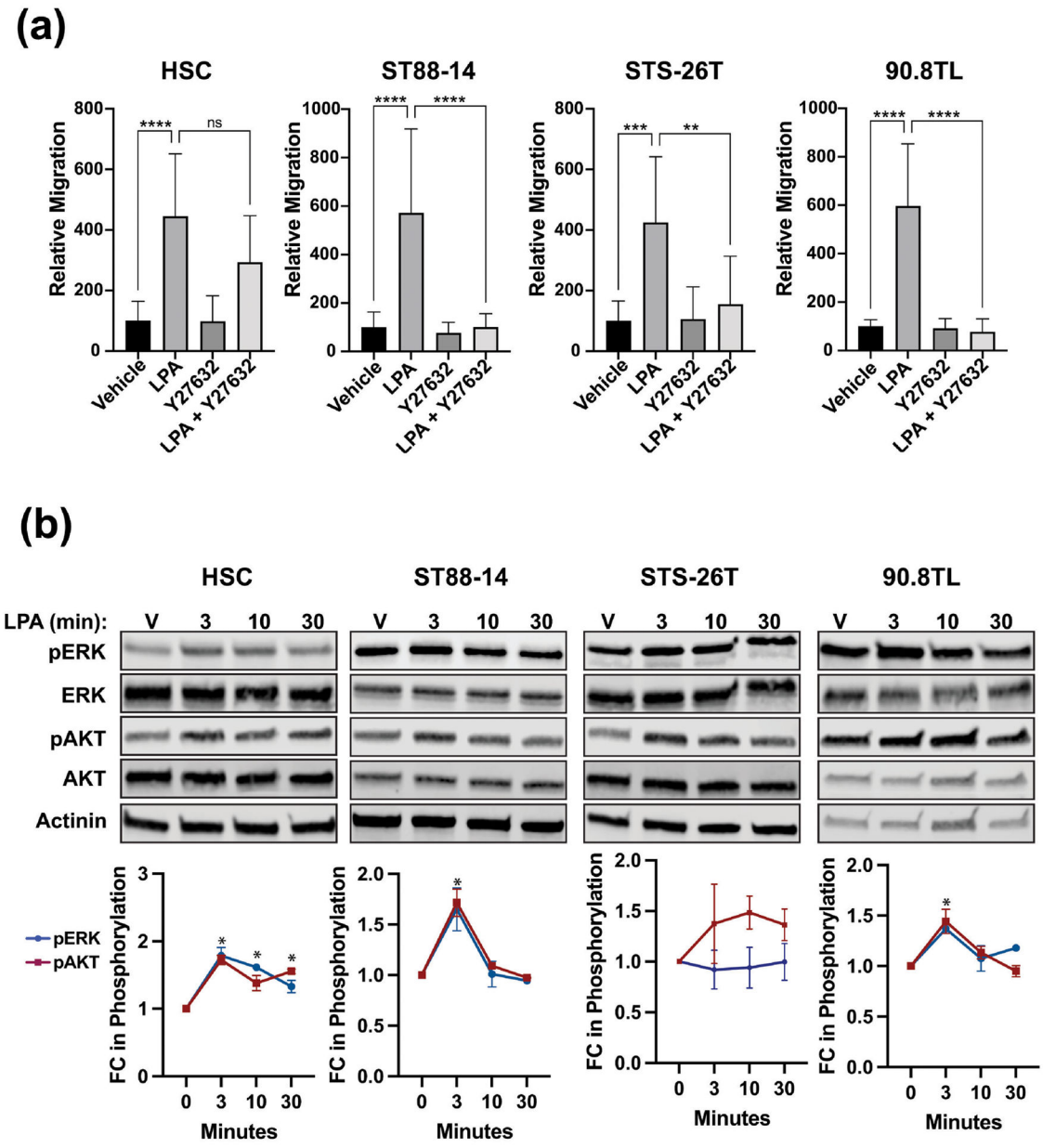

FIGURE 9.

Migration induced by oleoyl-LPA is ROCK-dependent. (a) Non-neoplastic human Schwann cells (HSC) and three human MPNST cell lines (ST88-14, STS-26T and 90.8TL) were challenged with vehicle, the concentration of LPA that optimally promotes migration, a 10 μM concentration of the selective ROCK inhibitor Y27632 or Y27632 plus LPA. Pretreatment with Y27632 significantly prevented LPA-enhanced migration of MPNST cells, but not that of non-neoplastic Schwann cells. (b) LPA stimulation of non-neoplastic Schwann cells and MPNST cells induced the phosphorylation of Erk. However, although LPA did not enhance phosphorylation of AKT in MPNST cells, it did modestly enhance AKT phosphorylation in non-neoplastic human Schwann cells. Quantification of the LPA induced fold change in ERK and AKT phosphorylation compared to total protein levels after

normalization to total protein is displayed in the graphs below the western blots. * indicates a p-value ≤0.05; ** indicates a p-value ≤0.005; *** indicates a p-value ≤0.0005.